Research Article

Chemical Review and Letters
journal homepage: www.chemrevlett.com
ISSN (online): 2645-4947 (print) 2676-7279

A theoretical study of X-H···C and X-H···π interactions between substituted benzene derivatives and HF, HCl, and HBr: AIM, NBO, and NMR analyses

Hala Bahir[1], Saad khudhur Mohammed[2], Afaa Mohammed Ibrahim[3], Ali Adhab Hussein[4], Azadeh Khanmohammadi[5, *]

[1] *Medical technical college, Al-Farahidi University, Iraq*
[2] *College of Dentistry, National University of Science and Technology, Dhi Qar, Iraq*
[3] *Department of Optical Techniques, Al-Noor University College, Iraq*
[4] *Department of Medical Laboratory Technics, Al-Zahrawi University College, Karbala, Iraq*
[5] *Department of Chemistry, Payame Noor University (PNU), P.O.Box 19395-4697, Tehran, Iran*

ARTICLE INFO

Article history:
Received 17 September 2023
Received in revised form 31 December 2023
Accepted 31 December 2023
Available online 26 October 2023

Keywords:
DFT
AIM
NBO
NMR
Aromaticity indices

ABSTRACT

The effects of X-H···C and X–H···π interactions are considered where the hydrogen acids act as a proton donor and the different π-systems such as para-substituted (H, F, Cl, OH, SH, CH_3, and NH_2) benzene derivatives act as a proton acceptor. The influence of substituents on the strength of interactions indicates that the electron-withdrawing groups weaken the interaction while electron-donating ones strengthen it. Topological properties of charge density show low ρ and positive $\nabla^2\rho_{BCP}$ values and these properties are typical for closed-shell interactions. Based on the obtained natural bond orbital analysis results, the greatest charge transfer occurs in the HF complexes, while the smallest of that belongs to the HBr ones. The aromaticity indicators are also examined upon complexation. Finally, the NMR data results exhibit that the maximum and minimum isotropic value of the proton shielding tensor corresponds to the HBr and HF complexes, respectively.

1. Introduction

Intermolecular forces play an essential role in explaining many phenomena in areas of modern chemistry, from molecular biology to supramolecular chemistry [1, 2]. An interesting aspect of these interactions in the biological field occurs when aromatic rings are involved, as they are present in many processes [3]. The most common non-covalent interactions involving aromatic rings are of π···π, XH···π, or ion···π type [4, 5]. Non-covalent or van der Waals interactions lead to the formation of a molecular cluster while covalent interactions lead to the formation of a classical molecule. As known, former interactions are much weaker than covalent bonds. The structure of liquids, solvation phenomena, molecular crystals [6], physisorption, and the structures of bio-macromolecules such as DNA and proteins [7, 8], and molecular recognition [9, 10] are a few phenomena determined by non-covalent interactions.

Non-covalent interactions have attracted much attention due to their extensive applications in the fields of chemistry, biology, and physics [11-19]. Hydrogen bond (H-bond) certainly holds the most important position among intermolecular interactions. It is demonstrated that the electrostatic interaction and induction and dispersion interactions contribute jointly to the formation of H-bonds [20]. Many theoretical studies on the structure, stability, and vibrational spectra employing ab initio and DFT calculations have been undertaken in recent years for the H-bonded complexes [21–25]. The H-bond chemical properties have both subtle and profound influences on the essential chemistry of life, crystal packing and engineering, self-assembly, solvation, catalysis, chelation, and a host of other essential phenomena.

The H-bond is a complex interaction that has at least four chemical characteristics: electrostatics (acid/base), polarization (hard/soft), van der Waals

∗ Corresponding author.; e-mail: az_khanmohammadi@yahoo.com
https://doi.org/10.22034/crl.2023.416728.1249

interaction (dispersion/repulsion), and covalency (charge transfer) [18]. The evidence for H-bond formation may be experimental or theoretical, or ideally, a combination of both [26]. There is a variety of H-bond interactions: those named as typical X–H···Y bridges between X (the proton donor) and Y (the proton acceptor) which are both electronegative atoms. The C–H···Y, X–H···C, and even C–H···C interactions are sometimes classified as unconventional H-bonds since very often the H-bond existence criteria are hardly accepted for them [27]. The π-cloud of an aromatic ring is now generally recognized as a weak H-bond acceptor [28]. It is also known that H–C groups engage in H-bonds with simple organic molecules [29]. The electrostatic nature of H-bonds suggests that nonmetal atoms other than hydrogen in a chemical functional group are capable of complementing an H-bond acceptor. Consequently, an uncharged non-reactive electrophile could have the potential to interact with an H-bond acceptor.

Experimental and theoretical results also indicate that weak interactions can be established between triple and double bonds, aromatic and cyclopropane rings, and X–H compounds (hydrogen halides, O–H, N–H, C–H derivatives, etc.). These interactions, which possess the essential properties of H-bonds, are usually called 'X–H···π hydrogen bonds' [30–32]. The properties of X–H···π hydrogen bonds are not only dependent on the properties of X, π-systems, and H but also are related to other factors such as substituent, hybridization, and solvation [33, 34]. There are numerous studies on X–H···π interactions which are often classified as H-bonds since π-electrons may be treated as proton acceptors (X–H designates the proton donating bond) [27]. Hence the X–H···π interactions have been the subject of extensive investigations, and their meaning for various chemical, physical, and biochemical processes was worked out in recent and earlier studies [35]. These interactions are common in crystal structures of organic and metalorganic compounds and their influence on the arrangement of molecules is often detected. The present study is directed to investigate the interactions of hydrogen acids (HX = HF, HCl, and HBr) with different π-systems such as benzene (A), 1,4-difluorobenzene (B), 1,4- dichlorobenzene (C), hydroquinone (D), benzene-1,4-dithiol (E), p-xylene (F), benzene-1,4-diamine (G) (see Fig. 1). In these complexes, the hydrogen acids are considered as proton donor and para-substituted (H, F, Cl, OH, SH, CH_3 and NH_2) benzene derivatives act as the proton acceptor. All the hydrogen acids are approximately perpendicular to the benzene rings in the selected structures.

The main objective of this article is to analyze the effects of X-H···C and X–H···π interactions on the geometrical features, the interaction energy, and the topological properties of benzene complexes substituted by electron-donating or electron-withdrawing groups. The DFT calculations are carried out for this analysis and AIM and NBO methods are applied. Furthermore, the complexation's effect on benzene derivatives' aromaticity is evaluated by calculating the corresponding aromaticity indices. Furthermore, to deal with this topic in depth, we comprehensively analyze the X-H···C and X–H···π interactions on NMR data in the studied complexes.

2. Computational Methods

All quantum chemical calculations are carried out with the Gaussian 09 [36] set of codes. Full geometry optimization is computed at the B3LYP-D/6-311++G(d,p) level of theory. For the investigated systems, the interaction energy (ΔE) is calculated by evaluating the difference between the total energy of complexes and individual monomers as given in Equation (1):

$$\Delta E = E_{complex} - (E_{HX} + E_{\pi\text{-system}}) \quad (1)$$

where ΔE is the intermolecular interaction energy, $E_{complex}$ is the total energy of complexes, and E_{HX} and $E_{\pi\text{-system}}$ are the total energies of hydrogen acid and para-substituted benzene monomers, respectively. The ΔE is corrected with the basis set superposition error (BSSE) [37]. Harmonic vibrational frequencies are estimated at the same level of theory on the optimized geometries to confirm the nature of the stationary points found and also to account for the zero-point vibrational energy (ZPVE) correction. The topological parameters are analyzed by the atoms in molecules (AIM) theory of Bader using AIM 2000 software [38]. Natural bond orbital (NBO) analysis [39] is carried out with the NBO program included in the Gaussian 09 package. Molecular orbital calculations such as the highest occupied molecular orbital (HOMO) and the lowest unoccupied molecular orbital (LUMO) are also performed on the investigated systems. The absolute NMR shielding values [40] are calculated using the Gauge-Independent Atomic Orbital (GIAO) method [41]. Herein, some spin–spin coupling constants ($^1J_{C–C}$, $^1J_{C–R'}$, and $^1J_{C–H}$) and the values of the proton shielding tensors are considered. The isotropic shielding values, $\sigma_{iso} = \frac{1}{3}(\sigma_{11} + \sigma_{22} + \sigma_{33})$ (σ_{ii} being the principal tensor components), are used to calculate the isotropic chemical shift δ with respect to TMS, $\delta_{iso}^{TMS} = (\sigma_{iso}^{TMS} - \sigma_{iso}^{X})$. On the other hand, the aromaticity of the benzene complexes and their derivatives is measured using several well-established indices of aromaticity such as the nucleus-independent chemical shift (NICS) [42], the harmonic oscillator model of aromaticity

(HOMA) [43], the para-delocalization index (PDI) [44] and the aromatic fluctuation index (FLU) [45]. In the present work, the R_{opt}, α, and δ_{ref} parameters for evaluation of HOMA and FLU indices are calculated at the B3LYP-D/6-311++G(d,p) level of theory (for CC bond: $R_{opt,CC}$ = 1.396 Å , α_{CC} = 88.54 and $\delta_{ref,CC}$ = 1.4).

3. Results and discussion

The optimized structures of the complexes that are named according to the position of the substitutions (R) on the benzene ring are depicted in Fig. 1. The computations propose that the type of hydrogen acid and the character of π-system are two dominant reasons that change the nature of the interaction. We have attempted to discuss the geometrical parameters, topological properties, and NBO analysis which describe the changes in the benzene ring during their interaction with hydrogen acids.

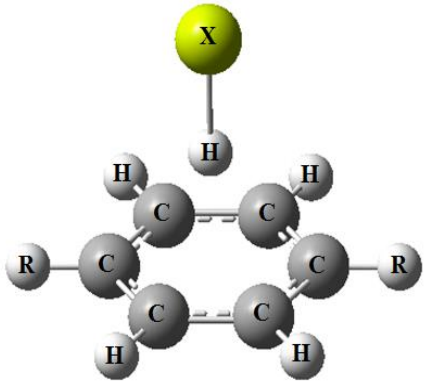

Fig. 1. The complexes of hydrogen acids with para-substituted (H, F, Cl, OH, SH, CH_3 and NH_2) benzene derivatives. **X** = F, Cl and Br, **R:** H = benzene (A), F = 1,4-difluorobenzene (B), Cl = 1,4 dichlorobenzene (C), OH = hydroquinone (D), SH = benzene-1,4-dithiol (E), CH_3 = p-xylene (F) and NH_2 = benzene-1,4-diamine (G).

3.1. Molecular geometry and interaction energy

The geometrical parameters and the values of interaction energy (ΔE) for the formed complexes between the hydrogen acids (HX = HF, HCl, and HBr) and different π-systems such as para-substituted (H, F, Cl, OH, SH, CH_3 and NH_2) benzene derivatives are shown in Table 1. Inspection of results reveals that the minimum and maximum interaction energies correspond to F and NH_2 substituents, respectively. The electronic properties of the substituents influence the strength of the attraction [46]. F, Cl, OH, and SH substitutions are σ-acceptors whereas CH_3 and NH_2 act as σ, π-donors. In the studied complexes, the electrostatic (inductive and resonance) effects of substitutions oppositely influence the interaction energies. The comparison of complexation energies indicates that the predominant factor in the NH_2-substituted ring is resonance (in comparison with induction). On the other hand, the F is an electronegative atom with induction predominate resonance. Thus, as seen in Table 1, the electron-withdrawing groups such as F and Cl weaken the interaction strength, while the electron-donating substituents (CH_3 and NH_2) strengthen it. It is obvious from Table 1 that the strength of interaction decreases in the following order: NH_2 > CH_3 > H > OH > SH > Cl > F for any given hydrogen acids.

For the studied complexes, the dependence between ΔE and $d_{H\cdots R}$ (the distance between the hydrogen of HX and the aromatic ring) should be considered. Theoretical results show that the $d_{H\cdots R}$ decrease is accompanied by the ΔE increase. As shown in Fig. 2, there is a good linear relationship between the values of ΔE and $d_{H\cdots R}$ with a correlation coefficient (R) equal to 0.911. Thus, $d_{H\cdots R}$ may be a useful parameter in describing the strength of the interactions. Furthermore, the geometrical parameters (see Table 1) indicate that HF establishes a shorter bond with the benzene ring than HCl and HBr. This fact depends essentially on the type of the acid's hydrogen; because the interactions decrease with an increase in the size of the halogen atom attached to the hydrogen for all complexes. Moreover, the nature of the interactions seems to be very similar for these three acids. This behavior is obvious for halogen atoms in the investigated acids; since they belong to the same group of the periodic table, the relative change in atomic radii for the halogen atom becomes greater as the size of the halogen atom increases.

Table 1. The interaction energies (ΔE, in kJ mol^{-1}), geometrical parameters (bond lengths (d), in Å), atomic charges (q, in e), and stretching frequencies (υ, in cm^{-1}) of H···R contact.

Complex	ΔE	d_{C-C}	d_{C-H}	$d_{C-R'}$ [a]	d_{H-X} [b]	$d_{H\cdots R}$	$q_{H\ (acidic)}$	q_X	υ
A-HF	-8.75	1.398	1.085	1.084	0.930	2.614	0.307	-0.278	109.20
A-HCl	-3.02	1.397	1.085	1.084	1.294	2.755	0.164	-0.141	70.52
A-HBr	-0.58	1.396	1.084	1.084	1.432	2.805	0.103	-0.103	51.87
B-HF	-1.07	1.397	1.083	1.351	0.928	2.680	0.311	-0.272	92.03
B-HCl	3.16	1.396	1.083	1.353	1.291	2.884	0.154	-0.128	56.58
B-HBr	4.73	1.394	1.083	1.354	1.430	2.967	0.077	-0.077	38.75
C-HF	-1.23	1.396	1.083	1.752	0.927	2.692	0.315	-0.275	80.99
C-HCl	3.09	1.393	1.082	1.754	1.290	2.895	0.156	-0.125	42.05
C-HBr	5.26	1.392	1.082	1.755	1.429	3.035	0.026	-0.052	35.89
D-HF	-7.37	1.397	1.084	1.370	0.931	2.602	0.336	-0.284	107.60
D-HCl	-1.57	1.395	1.083	1.371	1.293	2.673	0.175	-0.141	56.59
D-HBr	0.77	1.391	1.083	1.372	1.434	2.813	0.094	-0.093	52.92
E-HF	-4.95	1.401	1.085	1.784	0.929	2.635	0.333	-0.283	115.60
E-HCl	0.01	1.400	1.084	1.788	1.293	2.746	0.169	-0.140	56.41
E-HBr	2.63	1.399	1.084	1.789	1.431	2.814	0.034	-0.067	38.91
F-HF	-9.30	1.401	1.086	1.509	0.932	2.544	0.341	-0.292	109.20
F-HCl	-3.68	1.398	1.086	1.509	1.296	2.688	0.175	-0.148	75.04
F-HBr	-0.17	1.397	1.086	1.509	1.435	2.744	0.068	-0.089	57.62
G-HF	-12.50	1.402	1.086	1.403	0.934	2.564	0.365	-0.294	114.70
G-HCl	-5.53	1.402	1.085	1.405	1.295	2.674	0.233	-0.169	66.25
G-HBr	-2.24	1.400	1.085	1.407	1.435	2.680	0.131	-0.115	47.77

[a] R′ = H, F, Cl, O, S, C, N atoms in R substitution of A, B, C, D, E, F and G complexes, respectively.
[b] X = F, Cl, Br atoms in the hydrogen acids of A, B, C, D, E, F and G complexes.

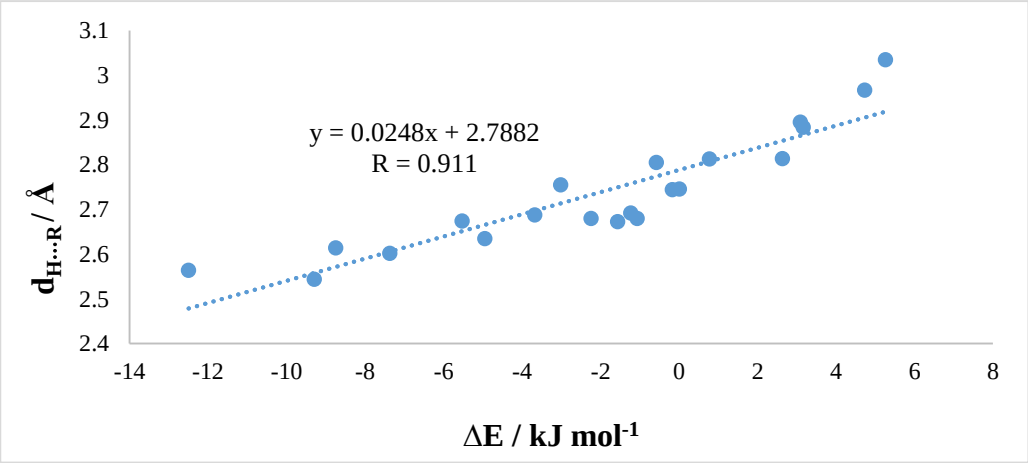

Fig. 2. Correlation between the ΔE and $d_{H\cdots R}$ values.

The change in other geometrical parameters of the studied complexes in the presence of interactions is also investigated. Our theoretical results show that the increase in the C-C (d_{C-C}) and C–H (d_{C-H}) bond lengths and also the decrease in the C–R′ bond length ($d_{C-R'}$) are accompanied with increasing in the absolute values of complexation energy (|ΔE|) (see Table 1). The atomic charges on the H (acidic) and X atoms ($q_{H(acidic)}$ and q_X) are also given in Table 1. As it is obvious from this Table, the X–H···π(C) interaction increases $q_{H(acidic)}$ values while decreasing q_X

amounts. In all the complexes, the computed binding strength varies with changing the ratio of charge to radius for the halogen atom attached to the hydrogen. Indeed, the increment in this ratio is associated with an increase in the interaction of the hydrogen acids and active sites in the benzene ring, and also enhancement in charge transfer from active sites to the hydrogen acids. Examination of our theoretical results reveals that the hydrogen acids act as proton donor centers and π-electrons of the para-substituted benzene rings act as the proton acceptors.

3.2. Vibrational frequency

Another index closely related to the strength of the interactions is the shifting of the H···R (hydrogen of HX with ring) stretching frequencies. Table 1 presents the stretching frequencies (υ) of the H···R contact for the investigated complexes. It is important to emphasize that with the strengthening of interaction energy, its stretching frequencies shift to upper wave numbers (see Table 1). As shown in this Table, the maximum and minimum stretching frequencies correspond to the HF and HBr complexes, respectively. Considering the results tabulated in Table 1 show that in most cases, upon substitution in the R position, the H···R stretching frequencies shift to lower wave numbers with respect to the unsubstituted complexes (A). Thus, performing such a comparison confirms that the interactions decrease during complexation.

Our calculations indicate that both the FH···R and the BrH···R stretching frequencies for the B complex appear red-shifted by ca. 17 cm^{-1} and 13 cm^{-1} with respect to those of the A complex, respectively. According to our theoretical results, the greatest shifts are observed for the electron-donating substitutions, while the smallest shifts correspond to the electron-withdrawing ones. For instance, the obtained results show that the FH···R stretching frequency for the G complex appears blue-shifted by ca. 5.5 cm^{-1} relative to the A complex, whereas the BrH···R stretching frequency for the G complex appears red-shifted by ca. 4 cm^{-1}. This result is associated with the shortening of the HF bond in the FH···R and the lengthening of the HBr bond in the BrH···R of the related complex.

3.3. AIM analysis

In Bader's topological QTAIM analysis [47], the nature of bonding interactions is analyzed in terms of the properties of electron density and its derivatives. Laplacian of ρ(r) is related to the bond interaction energy by a local expression of the virial theorem [38].

$$\left(\frac{\hbar^2}{4m}\right)\nabla^2\rho(r) = 2\,G(r) + V\,(r)$$

where G(r) is the electronic kinetic energy density, which is always positive, and V(r) is the electronic potential energy density and must be negative [48]. A positive value of Laplacian of ρ(r) shows a depletion of electronic charge along the bond. This is the case in a closed-shell electrostatic interaction. On the other hand, a negative value of Laplacian of ρ(r) indicates that electronic charge is concentrated in the internuclear region. This is the case in an electron-sharing (or covalent) interaction [49].

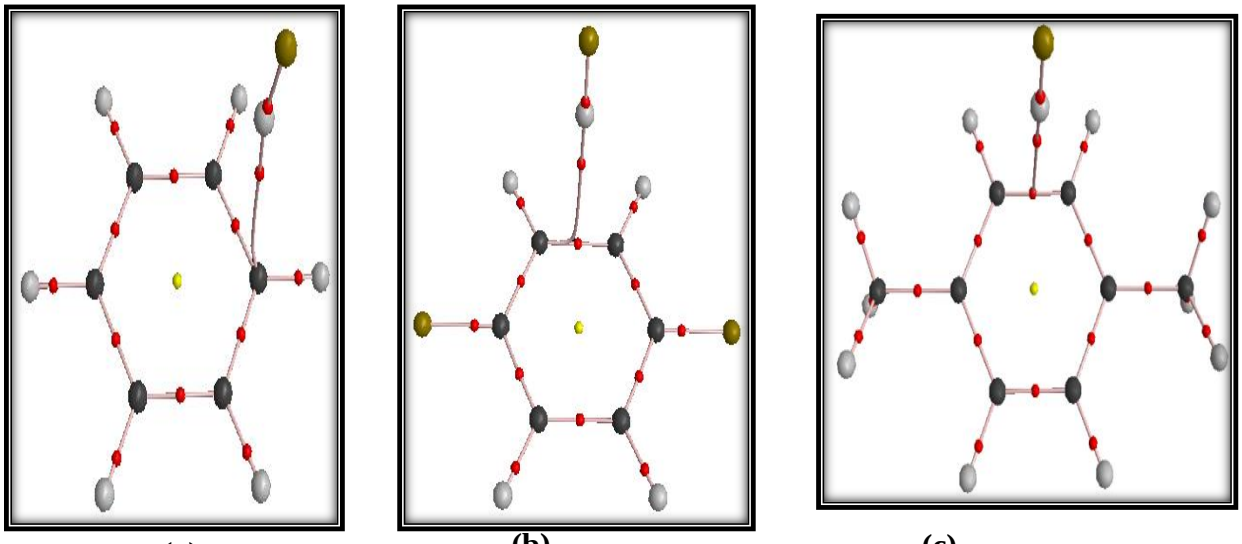

Fig. 3. Schematic representation of distribution of critical points in (a) A-HF, (b) B-HF and (c) F-HF complexes. Small red and yellow spheres, and lines represent bond critical points (BCPs), ring critical points (RCPs) and bond paths, respectively.

Table 2. The selected topological properties of electron density (in a.u.) obtained by AIM analysis.

Complex	ρ_{BCP}	$\nabla^2\rho_{BCP}$	$\rho_{C=C}$	ρ_{C-H}	$\rho_{C-R'}$	$\rho_{H\ (acidic)}$	$\rho_{R'}$
A-HF	0.0129	0.0375	0.3063	0.2821	0.2815	0.3135	0.9627
A-HCl	0.0097	0.0234	0.3072	0.2819	0.2815	0.7209	0.9673
A-HBr	0.0085	0.0195	0.3073	0.2819	0.2815	0.8965	0.9746
B-HF	0.0113	0.0340	0.3032	0.2821	0.2521	0.3158	9.6136
B-HCl	0.0079	0.0188	0.3042	0.2821	0.2509	0.7348	9.6176
B-HBr	0.0070	0.0158	0.3156	0.2819	0.2505	0.9129	9.6141
C-HF	0.0110	0.0329	0.3050	0.2835	0.1950	0.3154	17.1710
C-HCl	0.0069	0.0168	0.3094	0.2836	0.1941	0.7367	17.1791
C-HBr	0.0066	0.0150	0.3097	0.2833	0.1937	0.9056	17.1697
D-HF	0.0141	0.0415	0.3030	0.2813	0.2816	0.3166	9.0582
D-HCl	0.0088	0.0220	0.3082	0.2817	0.2804	0.7312	9.0649
D-HBr	0.0102	0.0235	0.3111	0.2812	0.2800	0.8915	9.0593
E-HF	0.0129	0.0381	0.3038	0.2818	0.1894	0.3134	15.8091
E-HCl	0.0091	0.0228	0.3046	0.2818	0.1881	0.7262	15.8203
E-HBr	0.0081	0.0195	0.3050	0.2819	0.1878	0.8984	15.7820
F-HF	0.0143	0.0421	0.3053	0.2803	0.2500	0.3135	5.9636
F-HCl	0.0107	0.0268	0.3061	0.2803	0.2498	0.7196	5.9636
F-HBr	0.0099	0.0237	0.3062	0.2803	0.2498	0.8898	5.9685
G-HF	0.0170	0.0462	0.3045	0.2787	0.2944	0.3156	8.0211
G-HCl	0.0101	0.0259	0.3048	0.2790	0.2929	0.7144	8.0187
G-HBr	0.0095	0.0231	0.3049	0.2790	0.2915	0.8842	8.0201

The molecular graphs of three complexes evaluated in this paper are presented in Fig. 3. The AIM analysis depicts one bond critical point between the interacting hydrogen and one carbon atom of the benzene ring in all complexes (except for F complexes). The BCP is made between the hydrogen atom and one π-bond of the benzene ring in CH_3-substituted complexes (see Fig. 3). In these complexes, the hydrogen acid is approximately perpendicular to the benzene rings and acts as a proton donor, whereas π-electrons of substituted benzene derivatives act as a proton acceptor. Table 2 shows the estimated topological parameters of the complexes. As observed in this Table, the interactions have low ρ (ranging from 0.0066 to 0.0170) and are also described by positive $\nabla^2\rho_{BCP}$ values (ranging from 0.0150 to 0.0462). These properties are typical for closed-shell interaction. Among all complexes, the obtained values for electron density (ρ_{BCP}) are the least for the interaction of the HBr with the substituted benzenes, while this interaction for the HF creates the greatest density at the BCP along the interaction line.

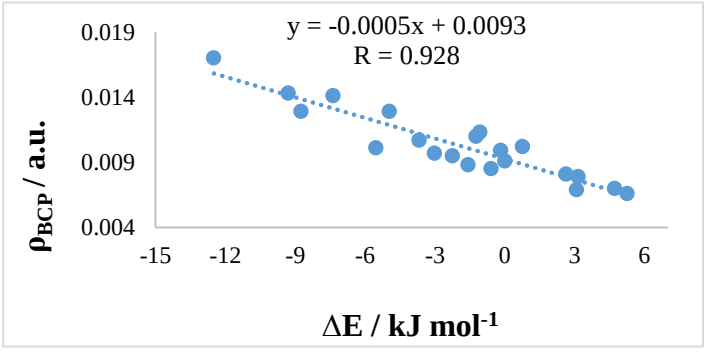

Fig. 4. Correlation between the ΔE and ρ_{BCP} values.

The changes of ρ at BCPs of C=C ($\rho_{C=C}$), C–R′ ($\rho_{C-R'}$), and C–H (ρ_{C-H}) bonds have been examined upon complexation. The results display that, in most cases, in the presence of X-H···C(π) interactions, the increase in |ΔE| is accompanied by the reduction in $\rho_{C=C}$, and also the increase in $\rho_{C-R'}$. A reverse relationship exists between the $\rho_{C=C}$ and $\rho_{C-R'}$ values and their corresponding bond lengths. Besides, a regular trend is not obtained between H···C(π) interactions and the electron density at the BCP of the C-H bond (see Table 2).

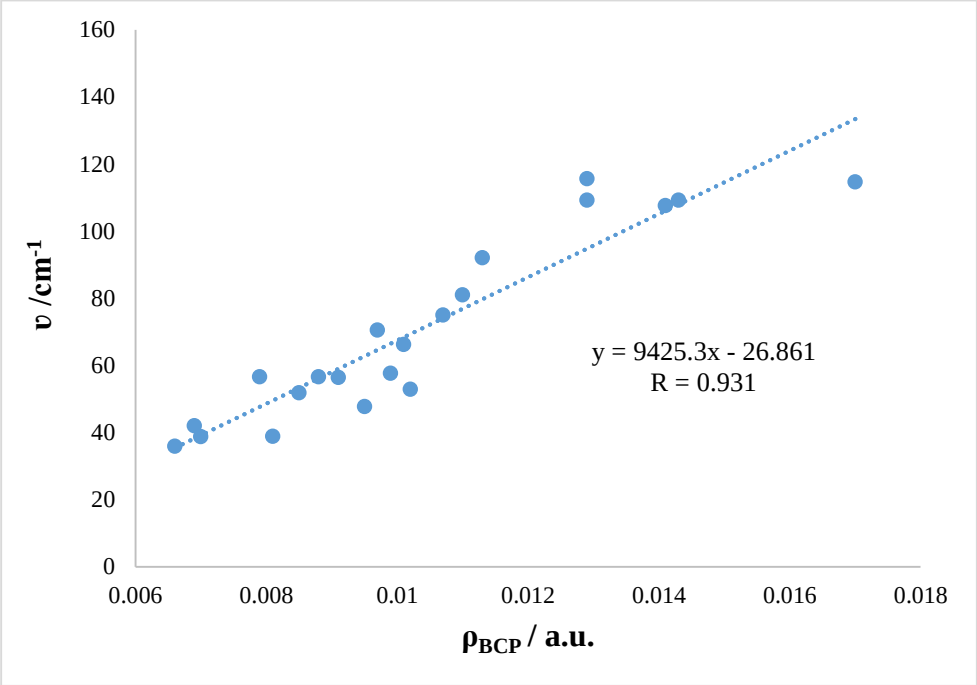

Fig. 5. Correlation between the υ and ρ_{BCP} values.

The changes in electron densities of acidic hydrogen and R′ atoms ($\rho_{H\ (acidic)}$ and $\rho_{R'}$) have also been considered upon complexation (see Table 2). These values are related to the electron density at the nuclear critical points. Our theoretical results confirm that the interaction between the hydrogen acids and benzene ring reduces the ρ_H values. Furthermore, a regular trend is not observed for the $\rho_{R'}$ values in the studied complexes. The correlation matrices for the ΔE, ρ_{BCP} and, υ parameters have also been investigated. There are good linear relationships between the interaction energies of complexes (ΔE) and vibrational frequencies (υ) with electron density at the BCP (ρ_{BCP}) with correlation coefficients (R) of equal to 0.928 and 0.931, respectively (see Figs. 4 and 5). Such consequences imply that the values of the bond critical point can be useful to estimate the strength of the interactions.

3.4. NBO analysis

The NBO method [39] demonstrates bonding concepts like atomic charge, Lewis structure, bond type, hybridization, bond order, charge transfer, and resonance possibility. The achieved outcomes are collected in Table 3. It can be seen that the most significant donor–acceptor interaction in the studied complexes is $\pi_{C=C\ (benzene)} \rightarrow \sigma^*_{H-X\ (hydrogen\ acid)}$ interaction. For the considered complexes, $\pi_{C=C}$ of the benzene ring and $\sigma^*_{H-X\ (hydrogen\ acid)}$ participate as donor and acceptor groups, respectively. Calculated interaction energies, $E^{(2)}$, lie in the range of 0.06 – 3.55 kcal mol^{-1}. Table 3 shows that, in most cases, the minimum and maximum values of $E^{(2)}$ correspond to the HBr and HF complexes, respectively.

Results of theoretical calculations in the HF complexes show that upon substitution the $E^{(2)}$ values decrease, which confirms that these interactions are stronger in the unsubstituted complexes (except for E and F complexes). As it is obvious from Table 3, the electron-withdrawing substituents (F and Cl) reduce the ability of the $\pi_{C=C}$ to donate electron density into the σ^*_{H-X} orbital and hence decrease the $E^{(2)}$ values and weaken the interactions, while it is vice versa for the electron-donating substituents (such as F and G). Therefore, our theoretical results show that in most cases, the trend in the donor-acceptor energies ($E^{(2)}$) is identical with |ΔE| and ρ_{BCP} parameters (see Tables 1-3).

Table 3. The values of $E^{(2)}$ correspond to $\pi_{(C=C)} \rightarrow \sigma^*_{(H-X)}$ interaction (in kcal mol^{-1}), occupation numbers of donor (ON_D) and acceptor (ON_A) orbitals and their corresponding energies and the charge transfers (Δq_{CT}, in e) in the studied complexes.

Complex	$\pi_{(C=C)} \rightarrow \sigma^*_{(H-X)}$	ON $_{(\pi\, CC)}$	ON $_{\sigma^*(HX)}$	E $_{(\pi\, CC)}$	E $_{\sigma^*(HX)}$	Δq_{CT}
A-HF	2.68	1.6816	0.0079	-0.2757	0.4212	0.029
A-HCl	1.78	1.6685	0.0090	-0.2671	0.1709	0.023
A-HBr	0.06	1.6607	0.0096	-0.2620	0.1051	0.000
B-HF	2.35	1.7064	0.0067	-0.3022	0.4116	0.039
B-HCl	0.43	1.6642	0.0065	-0.3000	0.1619	0.026
B-HBr	0.08	1.6667	0.0070	-0.2985	0.0961	0.000
C-HF	2.02	1.6859	0.0059	-0.3001	0.4124	0.040
C-HCl	0.76	1.6816	0.0034	-0.3035	0.1672	0.031
C-HBr	0.70	1.6783	0.0060	-0.3005	0.0963	-0.026
D-HF	1.05	1.6536	0.0102	-0.2796	0.4178	0.052
D-HCl	0.17	1.6504	0.0076	-0.2742	0.1698	0.034
D-HBr	0.07	1.6527	0.0139	-0.2727	0.1049	0.001
E-HF	2.79	1.7082	0.0080	-0.2881	0.4164	0.050
E-HCl	1.81	1.6799	0.0072	-0.2866	0.1685	0.029
E-HBr	1.76	1.6783	0.0078	-0.2840	0.1028	-0.033
F-HF	3.55	1.7000	0.0101	-0.2692	0.4211	0.049
F-HCl	0.84	1.6559	0.0114	-0.2558	0.1727	0.027
F-HBr	0.89	1.6557	0.0133	-0.2538	0.1073	-0.021
G-HF	2.43	1.6624	0.0135	-0.2634	0.4209	0.071
G-HCl	1.62	1.6555	0.0087	-0.2578	0.1803	0.064
G-HBr	0.16	1.7313	0.0110	-0.2557	0.1139	0.016

Table 3 shows the values of charge transfer (Δq_{CT}) for the investigated complexes. The amount of charge transfer between the substituted benzene rings and a hydrogen acid is easily determined as the difference between the total charge of HX in the isolated acids and the total charge of HX in the corresponding complexes. It can be seen from Table 3 that the greatest charge transfer (Δq_{CT}) occurs in the HF complexes, while the smallest of that belongs to the HBr complexes. These results can be supported by a more positive charge on the H atom in HF with respect to HCl and HBr in the related complexes. A positive charge on hydrogens of HF, HCl, and HBr in the NH_2-substituted complexes (0.365 |e|, 0.233 |e| and 0.131 |e|, respectively) demonstrates that these complexes transfer the smaller amounts of charge to the HCl and HBr than to HF. In the HF complexes, the smaller radius and the higher electron density on the F atom are accompanied by more charge transfer from the $\pi_{C=C}$ of the benzene ring to the HF. Fig. 6 displays the 3D NBO contour plot illustrating the interaction between the π bonding orbitals of C-C benzene with an antibonding orbital of HF (σ^*_{H-F}) in A-HF, B-HF, and G-HF complexes.

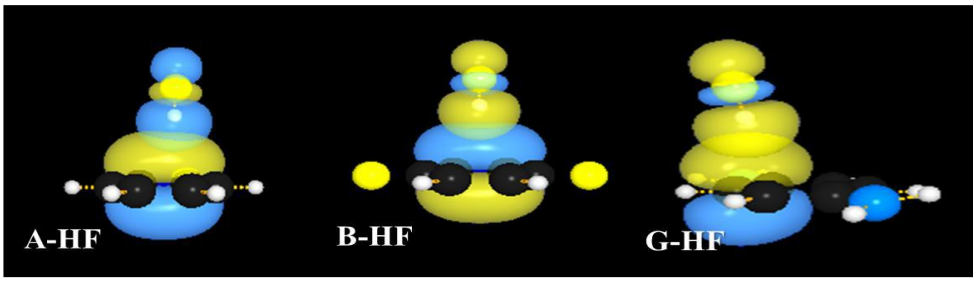

Fig. 6. NBO contour plots illustrating the interaction between the π bonding orbitals of C=C benzene with an antibonding orbital of HF in A-HF, B-HF and G-HF complexes.

3.5. NMR analysis

The isotropic value of the proton shielding tensors of benzene (benzenic IS) and acidic hydrogen (acidic IS), the isotropic chemical shifts of benzenic hydrogen (δ^{H}), and the acidic hydrogen (δ^{H^*}) of the studied complexes are gathered in Table 4. As shown in this Table, the maximum and minimum isotropic value of the proton shielding tensor corresponds to the HBr and HF complexes, respectively. This trend is reversed for the isotropic chemical shift of the H atom (δ^{H}). Similar results have been obtained for isotropic values of the proton shielding tensor of acidic hydrogen (acidic IS) except for C-HBr and D-HBr complexes. The substituents can also affect the isotropic value of the proton shielding tensor in the aforementioned complexes. For all substitutions, in comparison with the corresponding values of unsubstituted complexes, the isotropic value of the proton shielding tensor has been increased, while the isotropic chemical shift of the H atom (δ^{H}) has been decreased.

The meaningful correlations can be observed between the calculated NMR data and the other geometrical parameters. For instance, the relationship between the H shieldings and the $d_{H\cdots R}$ is reversed when the H shieldings are replaced by the chemical shifts (see Tables 1 and 4). Furthermore, the H···C(π) interactions decrease the isotropic value of the proton shielding tensors of benzene (benzenic IS) or acidic IS, so that the maximum |ΔE| value corresponds to the minimum H shieldings (except for C-HBr and D-HBr complexes due to acidic IS).

Table 4. Some NMR data calculated at the B3LYP-D/6-311++G** level of theory.

Complex	Benzenic IS (ppm)	δ^{H} (ppm)	Acidic IS (ppm)	δ^{H^*}[a] (ppm)	$^{1}J_{C-C}$ (Hz)	$^{1}J_{C-R'}$ (Hz)	$^{1}J_{C-H}$ (Hz)
A-HF	24.30	7.46	31.08	0.68	55.45	166.63	166.35
A-HCl	24.30	7.46	31.91	-0.15	56.72	166.27	166.27
A-HBr	24.33	7.43	32.18	-0.42	56.92	165.53	165.94
B-HF	24.80	6.96	31.17	0.59	73.58	-320.84	172.18
B-HCl	24.80	6.96	32.09	-0.33	74.06	-318.49	171.86
B-HBr	24.82	6.94	32.31	-0.56	74.52	-317.71	171.52
C-HF	24.56	7.20	31.11	0.64	67.24	-33.79	174.91
C-HCl	24.56	7.20	32.25	-0.49	67.32	-33.32	174.59
C-HBr	24.60	7.16	32.19	-0.43	67.74	-33.16	173.89
D-HF	24.92	6.84	30.49	1.26	66.01	23.23	168.88
D-HCl	25.00	6.76	31.99	-0.23	71.97	23.16	168.87
D-HBr	25.10	6.66	31.44	0.32	72.34	23.11	167.94
E-HF	24.85	6.91	30.79	0.97	58.45	-18.22	168.44
E-HCl	24.85	6.91	31.76	0.00	62.14	-17.82	168.19
E-HBr	24.89	6.87	31.95	-0.19	62.55	-17.68	168.00
F-HF	24.64	7.12	30.87	0.88	57.57	44.49	163.14
F-HCl	24.71	7.05	31.64	0.12	58.63	44.48	162.66
F-HBr	24.71	7.05	31.77	-0.02	58.84	44.50	162.63
G-HF	25.30	6.46	29.96	1.80	62.65	7.78	161.54
G-HCl	25.35	6.41	31.11	0.65	64.43	7.40	161.05
G-HBr	25.38	6.38	31.43	0.33	64.63	7.40	160.98

[a] δ^{H^*} (The isotropic chemical shift of the acidic hydrogen).

The substituent effect on the spin–spin coupling constants of $^{1}J_{C-C}$, $^{1}J_{C-R'}$, and $^{1}J_{C-H}$ has also been investigated (see Table 4). Most coupling constants (J) have positive values. With regard to Table 4, the values of $^{1}J_{C-C}$ increase by both electron-donating and electron-withdrawing substituents. In comparison with $^{1}J_{C-C}$, the substituent effect is reversed for $^{1}J_{C-R'}$ and $^{1}J_{C-H}$ (due to electron-donating substituents). The relationship between $^{1}J_{C-C}$, $^{1}J_{C-R'}$, and $^{1}J_{C-H}$ coupling constants and their corresponding bond lengths has also been investigated. In the analyzed complexes, the increase in C–C bond length (d_{C-C}) value is observed in the presence of H···C(π) interactions so that the shortest/longest d_{C-C} values correspond to HBr/HF complexes. The results also show that the decrease in the value of the $^{1}J_{C-C}$ is accompanied by a stretch of the C-C bond. As can be seen in Table 4,

the minimum and maximum values of $^1J_{C–C}$ correspond to the HF and HBr complexes, respectively. The influence of H···C(π) interaction on $^1J_{C–R'}$ has also been investigated in the present work. The results indicate that the C–R′ bond length ($d_{C–R'}$) decreases with the increase of interaction. The shortest/longest $d_{C–R'}$ values are observed when the benzene ring interacts with the HF/HBr. Similar to the $^1J_{C-C}$ trend, the increase in $d_{C–R'}$ is associated with the decrease in the absolute value of the $^1J_{C–R'}$ (except for the F-HBr complex). Thus, the change of $d_{C–R'}$ in the presence of the interactions strongly affects the $^1J_{C–R'}$ value. The $^1J_{C–H}$ is also affected by H···C(π) interactions. Our findings display that the H···C(π) interactions increase the $^1J_{C–H}$ value. The minimum and maximum values of the $^1J_{C–H}$ correspond to the HBr and HF complexes, respectively. The changes in C–H bond length ($d_{C–H}$) have been considered upon complexation. As shown in Table 4, a meaningful relationship exists between the $d_{C–H}$ and $^1J_{C–H}$ values; in this case, the $^1J_{C–H}$ enriches with the increase in the $d_{C–H}$.

3.6. Resonance parameters

For the studied systems, the indicators of local aromaticity such as HOMA, FLU, FLUπ, NICS (1), and PDI have been investigated. As shown in Table 5, the geometry-based HOMA values are very close to the ideal aromaticity index (HOMA = 1). Our theoretical results predict that the unsubstituted benzene is more aromatic than the substituted ones, irrespective of the π-donor or -acceptor character of the substituents. It is also apparent from Table 5 that the FLU and FLUπ indices for the unsubstituted complexes are smaller than those for the substituted ones. Our results show that the FLU and FLUπ values are close to zero (aromatic species) and nicely correlate together (R = 0.997), thus proving the similarity between FLU and FLUπ approaches. For investigated complexes, NICS (1) values are calculated below the center of the ring, on the opposite face to the hydrogen acids. The NICS index reveals that upon F substitution, the increment in aromaticity of benzene rings is accompanied by an increase in the NICS values with respect to the unsubstituted benzene (except for B-HCl). While the NICS values show unsubstituted complexes are less aromatic than the F-substituted ones, HOMA values indicate the higher aromaticity of these complexes. We state based on these results that HOMA provides an insight into benzene aromaticity, but this picture is not fully consistent with the NICS aromaticity model.

Table 5. Calculated aromaticity indices of the complexes.

Complex	HOMA	FLU	FLUπ	PDI	NICS (1)
A-HF	0.9998	0.0003	5E-06	0.1014	-8.2724
A-HCl	0.9999	0.0004	3E-06	0.1015	-9.9250
A-HBr	0.9998	0.0005	2E-06	0.1016	-9.8973
B-HF	0.9955	0.0025	8E-05	0.0934	-10.0127
B-HCl	0.9951	0.0454	0.0276	0.1016	-9.7646
B-HBr	0.9950	0.0029	0.0002	0.0938	-10.0306
C-HF	0.9990	0.0019	0.0001	0.0930	-9.4485
C-HCl	0.9988	0.0019	6E-05	0.0937	-9.6302
C-HBr	0.9987	0.0021	0.0001	0.0936	-9.7175
D-HF	0.9995	0.0037	0.0005	0.0895	-8.6356
D-HCl	0.9994	0.0040	0.0004	0.0902	-8.7660
D-HBr	0.9995	0.0044	0.0006	0.0876	-8.9119
E-HF	0.9990	0.0021	0.0002	0.0901	-8.3054
E-HCl	0.9987	0.0021	0.0002	0.0907	-8.4660
E-HBr	0.9987	0.0024	0.0002	0.0906	-8.5357
F-HF	0.9992	0.0480	0.0264	0.1038	-9.1670
F-HCl	0.9992	0.0468	0.0272	0.1039	-9.5053
F-HBr	0.9992	0.0453	0.0269	0.1038	-9.7029
G-HF	0.9977	0.0044	0.0004	0.0870	-8.2049
G-HCl	0.9979	0.0044	0.0006	0.0876	-8.2067
G-HBr	0.9980	0.0047	0.0005	0.0876	-8.4508

The calculated NICS (1) values also show that the HF complexes have the least aromaticity (except for the B complex) whereas the greatest aromaticity is obtained for the HBr complexes (except for the A complex). Furthermore, the results of Table 5 confirm that the aromaticity depends on the type of the substituent. The NICS values for the electron-withdrawing substituents (F and Cl) are more negative than the electron-donating ones (CH_3 and NH_2). Therefore, the latter cases become less effective in the improvement of the aromaticity than the formers.

The other index to be evaluated here is the PDI descriptor [45]. Our theoretical results based on the PDI index, predict unsubstituted benzene to be more aromatic than the substituted ones (except for F complexes). There is a satisfactory correspondence between PDI, HOMA, FLU, and FLUπ indices. In general, larger PDIs go with larger values of HOMA and lower FLU and FLUπ values (see Table 5).

3.7. HOMO–LUMO analysis

Molecular orbitals including the highest occupied molecular orbital (HOMO) and the lowest unoccupied molecular orbital (LUMO) are useful parameters for predicting the most reactive position in conjugated systems [50]. While the HOMO energy is directly related to the ionization potential, the LUMO energy corresponds directly to the electron affinity [51, 52]. The energy difference between HOMO and LUMO, referred to as the energy gap (ΔE_{H-L}), is a critical parameter for determining molecular electrical transport properties because it is a measure of electron conductivity.

Table 6. Molecular orbital properties including energy gap (ΔE_{H-L}), chemical hardness (η), softness (S) and chemical potential (μ) in terms of eV, and changes in thermodynamic functions (kJ mol^{-1}) upon complex formation.

Complex	ΔE_{H-L}	η	S	μ	ΔH°	ΔG°	$T\Delta S^\circ$
A-HF	6.552	3.276	0.305	-4.273	-2.578	31.732	-34.270
A-HCl	6.545	3.273	0.306	-4.159	0.869	23.989	-23.244
A-HBr	6.534	3.267	0.306	-4.112	1.087	22.017	-20.860
B-HF	5.852	2.926	0.342	-4.593	0.213	23.519	-23.244
B-HCl	5.868	2.934	0.341	-4.461	1.221	21.660	-20.562
B-HBr	5.858	2.929	0.341	-4.417	1.638	20.781	-19.072
C-HF	5.685	2.842	0.352	-4.494	0.352	24.593	-24.138
C-HCl	5.756	2.878	0.347	-4.368	1.567	22.495	-20.860
C-HBr	5.706	2.853	0.351	-4.343	1.651	20.663	-19.072
D-HF	5.125	2.562	0.390	-3.729	-0.609	27.001	-27.714
D-HCl	5.189	2.594	0.386	-3.611	0.439	26.334	-25.926
D-HBr	5.107	2.553	0.392	-3.609	0.630	26.596	-25.926
E-HF	4.848	2.424	0.413	-3.801	-0.536	28.366	-28.906
E-HCl	4.894	2.447	0.409	-3.728	0.801	25.037	-24.138
E-HBr	4.911	2.456	0.407	-3.685	0.929	26.552	-25.628
F-HF	6.007	3.004	0.333	-3.867	1.289	25.302	-24.138
F-HCl	6.023	3.011	0.332	-3.765	2.762	22.062	-19.370
F-HBr	6.013	3.006	0.333	-3.729	2.888	21.316	-18.476
G-HF	4.576	2.288	0.437	-3.104	-0.990	27.870	-28.906
G-HCl	4.671	2.336	0.428	-2.997	0.481	25.809	-25.330
G-HBr	4.565	2.283	0.438	-2.992	0.585	27.405	-26.820

In the present study, the HOMO and LUMO energies are calculated using the B3LYP-D method and 6-311++G(d,p) basis set. The plots of HOMO and LUMO are drawn in Fig. 7. All the HOMO and LUMO orbitals have nodes. The nodes in each HOMO and LUMO are placed symmetrically. The positive phase is red and the negative one is green. According to Fig. 7, the charge density of HOMO is localized over the ring of the entire complexes (except for H atoms and HF). By contrast, the LUMO is characterized by a charge distribution on all

structures. It also shows the antibonding character at C-F, C-N, and N-H bonds. In other words, there is no electronic projection over the F and NH_2 groups of the ring and HF. In Fig. 7, the energy gap is calculated at 6.55, 5.85, and 3.37 eV for A-HF, B-HF, and G-HF complexes, respectively. It can be mentioned that the lower the HOMO and LUMO energy gap explains the eventual charge transfer interactions taking place within the molecule.

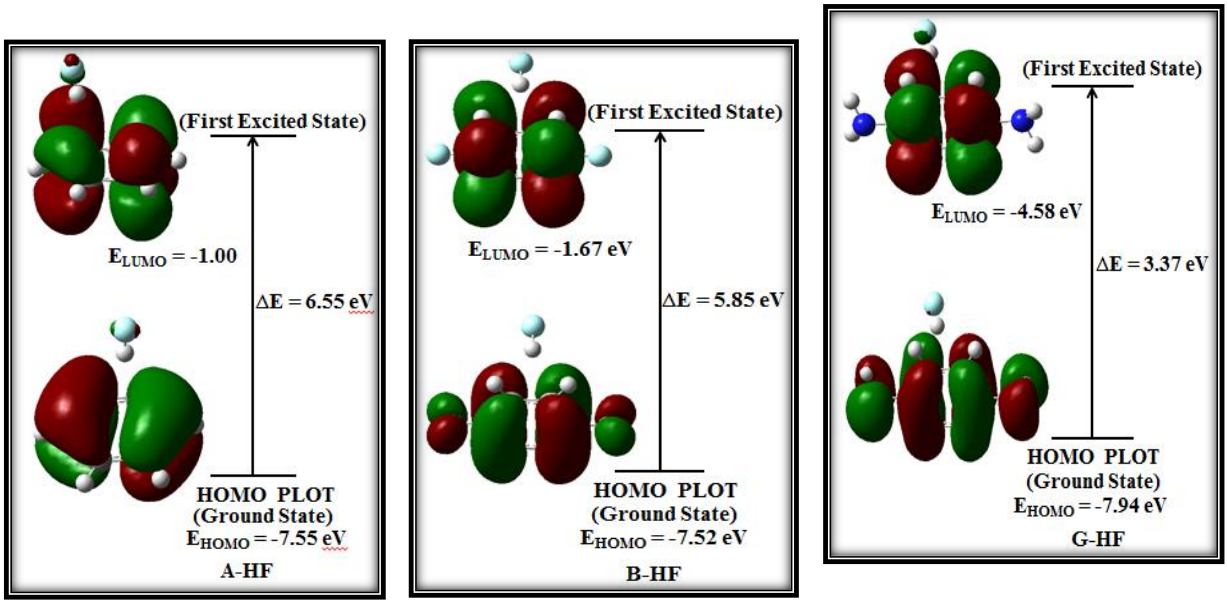

Fig. 7. HOMO and LUMO of A-HF, B-HF and G-HF complexes as obtained at the B3LYP-D/6-311++G(d,p) level of theory.

For the closed-shell molecules, the global chemical reactivity descriptors such as hardness (η), electronic chemical potential (μ), and softness (S) [53–57] are defined using Koopman's theorem as follows:

$$\eta = \frac{(I - A)}{2} \quad (3)$$

$$\mu = \frac{-(I + A)}{2} \quad (4)$$

where I and A are the ionization potential and electron affinity of the compounds, respectively. These quantities can be expressed through HOMO and LUMO energies as $I = -E_{HOMO}$ and $A = -E_{LUMO}$. Furthermore, softness is a property of molecules that measures the extent of chemical reactivity. It is the reciprocal of hardness.

$$S = \frac{1}{\eta} \quad (5)$$

In this study, the chemical hardness and electronic chemical potential of the studied species are given in Table 6. The molecules having large energy gaps are known as hard and molecules having small energy gaps are known as soft molecules. The obtained results show that the chemical hardness of the unsubstituted complexes (A) is greater than the substituted ones, which indicates these complexes are more stable than the others. On the other hand, the molecules with the least HOMO-LUMO gap are more reactive. From the calculations, it can be observed that the G and E complexes belong to soft materials. Moreover, as seen in Table 6, the obtained chemical potential values are negative, so all complexes are stable. The results display that the chemical potential of the HBr complexes is greater than the others. Furthermore, our findings confirm that the values of chemical potential for the studied complexes increase by the electron-donating substituents (such as F and NH_2) and decrease by the electron-withdrawing ones (F and Cl).

3.8. Thermodynamic parameters

The thermodynamic functions of enthalpy (ΔH°), Gibbs free energy (ΔG°), and entropy (ΔS°) from spectroscopic data are obtained at a temperature of 298.15 K and one atmospheric pressure. It can be stated that the complexes with lower standard Gibbs energy of formation are relatively more stable, whereas those with a higher relatively standard energy of formation are more unstable. The calculated thermodynamic properties of the complexes are available in Table 6. The values of the standard enthalpies show that the formation of A-HF, D-HF, E-HF, and G-HF complexes are enthalpically favored (exothermic), whereas these values in other complexes are enthalpically disfavored (endothermic). The values of

$T\Delta S°_{298}$ implied the large entropy changes during the formation of complexes. In some cases, the high negative values of $T\Delta S°_{298}$ determine the positive values of $\Delta G°_{298}$. The formation of several systems requires a larger entropy than energy changes (in other words $|T\Delta S°_{298}| > |\Delta H°_{298}|$).

In the studied complexes, ΔG values are positive ($\Delta G° > 0$). Therefore, the formation of the complexes is thermodynamically disfavored. Since $\Delta S° < 0$ and $|T\Delta S°| > |\Delta H°|$), hence the entropic factor controls the stability of the complexes. The obtained results in this study show that all of the thermodynamic properties are greatly dependent on the nature of the R substituents and the type of hydrogen acids. The data reveal that the HF/HBr hydrogen acids increase/decrease the stability of all complexes more than the HCl ones. Thus, the HF complexes are characterized by the higher ΔG° values. The electronic properties of the substituents also influence the thermodynamic parameters. According to our theoretical results on the HF complexes, the greatest stability is enthalpically observed for the unsubstituted complex (A) and HF complexes substituted with OH, SH, and NH_2 groups (D, E, and G complexes). Hence, these complexes are characterized by the lower ΔH° values.

3.9. Molecular electrostatic potential

The molecular electrostatic potential (MEP) provides a visual representation of the chemically active sites and comparative reactivity of atoms. The MEP at a point around a molecule indicates the net electrostatic effect produced at that point by the total charge distribution (electron + proton) of the molecule and correlates with dipole moments, electronegativity, partial charges, and chemical activity of the molecules. The different values of the electrostatic potential at the surface are represented by different colors; red represents regions of most negative electrostatic potential, blue signifies regions of most positive electrostatic potential and green characterizes regions of zero potential. Potential increases in the order red < orange < yellow < green < blue. In the present study, MEP 3D plots of the benzene and the para-substituted (F and NH_2) derivatives with HF hydrogen acid are drawn in Fig. 8.

Regions of negative V(r) are usually associated with the lone pair of electronegative atoms. As seen from the MEP map of the studied complexes, the regions having the negative potential are over the electronegative atom (F atom) and the plane of the benzene ring. The three-dimensional electrostatic potential profile of G-HF indicates a complete cover of the aromatic ring with negative potential, whereas in B-HF the negative potential cover is partial. The aromatic ring in the complex of benzene (A-HF) is completely devoid of negative potential (see Fig. 8). The regions having the positive potential are the hydrogen atoms of the benzene ring (indicated by the deepest blue color), indicating that these sites can be the most probably involved in nucleophilic processes. Consequently, the position of the HF hydrogen acid is tilted closer toward the plane of the benzene ring in the equilibrium geometry of the G-HF complex, whereas the HF remains over the aromatic ring in the B-HF complex.

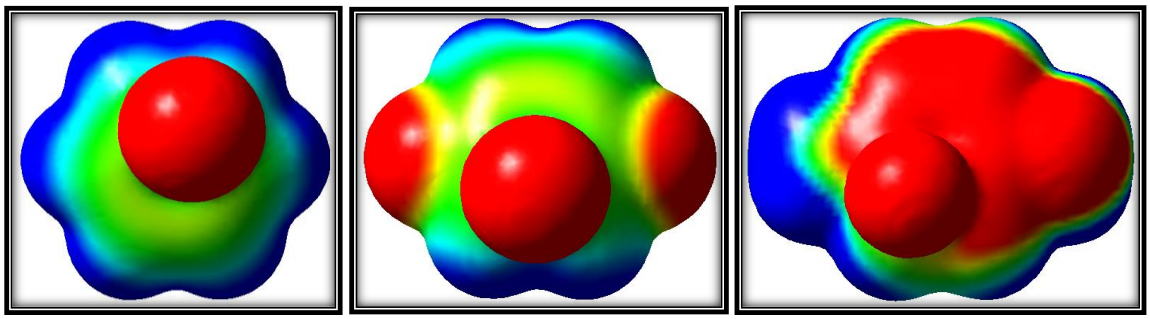

Fig. 8. Electron density isosurfaces for A-HF, B-HF and G-HF complexes calculated by B3LYP-D method and 6-311++G(d,p) basis set.

4. Conclusions

In the present study, we have investigated the effects of structural and electronic of the hydrogen acids (HF, HCl, and HBr) with different π-systems such as the para-substituted (H, F, Cl, OH, SH, CH_3, and NH_2) benzene derivatives using DFT method. The results show that the strongest interactions are related to the HF complexes, while the weakest correspond to the HBr ones. Our findings also reveal that the electron-withdrawing groups weaken the interactions while electron-donating ones strengthen them. These interactions have low ρ and are also characterized by positive $\nabla^2\rho_{BCP}$ values that these properties are typical for closed-shell interactions. The results of NBO analysis display that the greatest charge

transfer occurs in the HF complexes, while the smallest of that belongs to the HBr ones, which are in agreement with their obtained $E^{(2)}$ energies. From NMR analysis, it can be seen that the maximum and minimum isotropic value of the proton shielding tensor corresponds to the HBr and HF complexes, respectively. This trend is reversed for the isotropic chemical shift of the H atom. The analysis of molecular orbitals shows that the chemical hardness of the unsubstituted complexes is greater than the substituted ones, which indicates these complexes are more stable than the others. Our theoretical results based on HOMA, FLU, and FLUπ indices, predict unsubstituted benzene to be more aromatic than the substituted ones.

Acknowledgements

The authors wish to thank the Payame Noor University, Tehran, Iran for its support.

References

[1] P. Hobza, R. Zaradnik, Intermolecular complexes; the role of van der Waals systems in physical chemistry and the biodisciplines, Elsevier, Amsterdam (1988).
[2] I. Kaplan, Intermolecular interactions, physical picture, computational methods and model potentials, John Wiley & Sons, Chichester (2006).
[3] E. A. Meyer, R. K. Castellano, F. Diederich, Interactions with aromatic rings in chemical and biological recognition. Angew. Chem. Int. Ed. 42 (2003) 1210.
[4] S. Tsuzuki, T. Uchimaru, Magnitude and physical origin of intermolecular interactions of aromatic molecules: recent progress of computational studies. Curr. Org. Chem. 10 (2006) 745.
[5] J. C. Ma, D. A. Dougherty, The cation-π interaction. Chem. Rev. 97 (1997) 1303.
[6] I. Geronimo, E. C. Lee, N. J. Singh, K. S. Kim, How different are electron-rich and electron-deficient π interactions? J. Chem. Theory Comput. 6 (2010) 1931.
[7] P. Tarakeshwar, H. S. Choi, K. S. Kim, Olefinic vs aromatic π- h interaction: a theoretical investigation of the nature of interaction of first-row hydrides with ethene and benzene. J. Am. Chem. Soc. 123 (2001) 3323.
[8] E. C. Lee, B. H. Hong, J. Y. Lee, J. C. Kim, D. Kim, Y. Kim, P. Tarakeshwar, K. S. Kim, Substituent Effects on the Edge-to-Face Aromatic Interactions. J. Am. Chem. Soc. 127 (2005) 4530.
[9] K. S. Kim, P. Tarakeshwar, J. Y. Lee, Molecular clusters of π-systems: theoretical studies of structures, spectra, and origin of interaction energies. Chem. Rev. 100 (2000) 4145.
[10] M. O. Sinnokrot, C. D. Sherrill, Highly accurate coupled cluster potential energy curves for the benzene dimer: sandwich, T-shaped, and parallel-displaced configurations. J. Phys. Chem. A 108 (2004) 10200.
[11] S. Scheiner, Hydrogen bonding. a theoretical perspective, Oxford University Press, New York (1997).
[12] A. Siadati, A theoretical study on the possibility of functionalization of C20 fullerene via its Diels-Alder reaction with 1, 3-butadiene. Lett. Org. Chem. 13(1) (2016) 2.
[13] S. A. Siadati, Effect of steric congestion on the stepwise character and synchronicity of a 1, 3-dipolar reaction of a nitrile ylide and an olefin. J. Chem. Res. 39(11) (2015) 640.
[14] A. R. Bekhradnia, S. Arshadi, S. A. Siadati, 1, 3-Dipolar cycloaddition between substituted phenyl azide and 2, 3-dihydrofuran. Chem. Pap. 68 (2014) 283.
[15] F. Alirezapour, M. Mohammadi, A. Khanmohammadi, Exploration of the mutual effects between cation–π and intramolecular hydrogen bond interactions in the different complexes of mesalazine with metal cations of alkali and alkaline-earth: A DFT study. Chem. Rev. Lett. 6 (2023) 262.
[16] M. Javdani Zamani Sagheb, L. Hokmabady, A. Khanmohammadi, A comprehensive investigation into the effect of substitution on electronic structure, charge transfer, resonance, and strength of hydrogen bond in 3–amino-propene thial and its analogous: A DFT calculation. Chem. Rev. Lett. 6 (2023) 308.
[17] M. Koohi, H. Bastami, Investigation of Ti-B nanoheterofullerenes evolved from C20 nanocage through DFT. Chem. Rev. Lett. 6 (2023) 223.
[18] A. Yadav, A. Taha, Y. A. Abdulsayed, S. M. Saeed, Adsorption of a biological active ethionamide over the Surface of a Fe- porphyrin induced carbon nancone (Fe-PICNC) system Through a Density Functional Theory (DFT). Chem. Rev. Lett. 6 (2023) 128.
[19] F. Iorhuna, A. Shehu Muhammad, A. M. Ayuba1, N. Aondofa Thomas, Molecular Dynamic Simulations and Quantum Chemical Studies of Nitrogen Based Heterocyclic Compounds as Corrosion Inhibitors on Mild Steel Surface. Chem. Rev. Lett. 6 (2023) 114.
[20] Z. Czyznikowska, On the importance of electrostatics in stabilization of stacked guanine–adenine complexes appearing in B-DNA crystals. J. Mol. Struct. (Theochem) 895 (2009) 161.
[21] D. Hadzi, Theoretical treatment of hydrogen bonding, Wiley, New York (1997).
[22] J. E. Del Bene, I. Shavitt, Intermolecular interaction. from van der Waals to strongly bound complexes, Wiley, New York (1997).
[23] A. Zabardasti, A. Kakanejadifard, A. A. Hoseini, M. Solimannejad, Competition between hydrogen and dihydrogen bonding: interaction of B_2H_6 with CH_3OH and $CH_nX_{3-n}OH$ derivatives. Dalton. Trans. 39 (2010) 5918.
[24] H. Roohi, A. R. Nowroozi, E. Anjomshoa, H-bonded complexes of uracil with parent nitrosamine: a quantum chemical study. Comput. Theor. Chem. 965 (2011) 211.
[25] O. V. Shishkin, I. S. Konovalova, L. Gorb, J. Leszczynski, Novel type of mixed O–H···N/O–H···π hydrogen bonds: monohydrate of pyridine. Struct. Chem. 20 (2009) 37.
[26] G. R. Desiraju, A Bond by Any Other Name. Angew. Chem. Int. Ed. Engl. 50 (2011) 52.
[27] G. R. Desiraju, T. Steiner, The Weak Hydrogen Bond in Structural Chemistry and Biology, Oxford University Press, Oxford (1999).
[28] (a) G. W. Gokel, S. L. De Wall, E. S. Meadows, Experimental evidence for alkali metal cation-π interactions.

Eur. J. Org. Chem. 7 (2000) 2967. (b) J. P. Gallivan, D. A. Dougherty, Can Lone Pairs Bind to a π System? The Water···Hexafluorobenzene Interaction. Org. Lett. 1 (1999) 103. (c) E. Kim, W. Paliwal, C. S. Wilcox, Measurements of Molecular Electrostatic Field Effects in Edge-to-Face Aromatic Interactions and CH-π Interactions with Implications for Protein Folding and Molecular Recognition. J. Am. Chem. Soc. 120 (1998) 11192.

[29] (a) R. D. Green, Hydrogen Bonding by C–H Groups, Macmillan, London (1974). (b) R. Vargas, J. Garza, D. A. Dixon, B. Hay, How Strong Is the C^{α}–H···OC Hydrogen Bond? J. Am. Chem. Soc. 122 (2000) 4750.

[30] T. H. Tang, W. J. Wu, Y. P. Yu, A quantum chemical study on selected π-type hydrogen-bonded systems. J. Mol. Struct. THEOCHEM 207 (1990) 319.

[31] T. Steiner, Cooperative C≡C–H···C≡C–H interactions: crystal structure of DL-prop-2-ynylglycine and database study of terminal alkynes. J. Chem. Soc. Chem. Commun. 1 (1995) 95.

[32] I. Rozas, I. Alkorta, J. Elguero, Unusual Hydrogen Bonds: H···π Interactions. J. Phys. Chem. A 101 (1997) 9457.

[33] P. Hobza, Z. Havlas, Blue-shifting hydrogen bonds. Chem. Rev. 100 (2000) 4253.

[34] A. D. Buckingham, J. E. Del Bene, S. A. C. McDowell, The hydrogen bond. Chem. Phys. Lett. 463 (2008) 1.

[35] S. J. Grabowski (Ed.), J. Leszczynski (Ed.), Challenges and Advances in Computational Chemistry and Physics, Springer (2006).

[36] M. J. Frisch, G. W. Trucks, H. B. Schlegel, G. E. Scuseria, M. A. Robb, J. R. Cheese-man, G. Scalmani, V. Barone, B. Mennucci, G. A. Petersson, H. Nakatsuji, M. Caricato, X. Li, H. P. Hratchian, A. F. Izmaylov, J. Bloino, G. Zheng, J. L. Son-nenberg, M. Hada, M. Ehara, K. Toyota, R. Fukuda, J. Hasegawa, M. Ishida, T. Nakajima, Y. Honda, O. Kitao, H. Nakai, T. Vreven, J. A. Montgomery Jr, J. E. Peralta, F. Ogliaro, M. J. Bearpark, J. Heyd, E. N. Brothers, K. N. Kudin, V. N. Staroverov, R. Kobayashi, J. Normand, K. Raghavachari, A. P. Rendell, J. C. Bu-rant, S. S. Iyengar, J. Tomasi, M. Cossi, N. Rega, N. J. Millam, M. Klene, J. E. Knox, J. B. Cross, V. Bakken, C. Adamo, J. Jaramillo, R. Gomperts, R. E. Stratmann, O. Yazyev, A. J. Austin, R. Cammi, C. Pomelli, J. W. Ochterski, R. L. Martin, K. Mo-rokuma, V. G. Zakrzewski, G. A. Voth, P. Salvador, J. J. Dannenberg, S. Dapprich, A. D. Daniels, Ö. Farkas, J. B. Foresman, J. V. Ortiz, J. Cioslowski, D. J. Fox, Gaussian 09, Gaussian, Inc., Wallingford, CT, USA (2009).

[37] S. B. Boys, F. Bernardi, The calculation of small molecular interactions by the differences of separate total energies. Some procedures with reduced errors. Mol. Phys. 19 (1970) 553.

[38] R. F. W. Bader, A bond path: a universal indicator of bonded interactions. J. Phys. Chem. A 102 (1998) 7314.

[39] B. K. Paul, S. Mahanta, R. B. Singh, N. Guchhait, A DFT-Based Theoretical Study on the Photophysics of 4-Hydroxyacridine: Single-Water-Mediated Excited State Proton Transfer. J. Phys. Chem. A 114 (2010) 2618.

[40] P. Pulay, J. F. Hinton, K. Wolinski, in: J. A. Tossel (Ed), Nuclear magnetic shieldings and molecular structure, Kluwer, Dordrecht (1993).

[41] W. J. Hehre, L. Radom, P. R. Schleyer, J. A. Pople, Ab Initio Molecular Orbital Theory, Wiley, New York (1986).

[42] M. K. Cyranski, T. M. Krygowski, A. L. Katritzky, P. v. R. Schleyer, To what extent can aromaticity be defined uniquely? J. Org. Chem. 67 (2002) 1333.

[43] A. Mrozek, J. Karolak-Wojciechowska, P. Amiel, J. Barbe, Five-membered heterocycles. Part II. Crystal structures and HOMA index calculations for selected 1,3,4-thiadiazole derivatives. J. Mol. Struct. 524 (2000) 159.

[44] J. Poater, M. Duran, M. Sola, B. Silvi, Theoretical evaluation of electron delocalization in aromatic molecules by means of atoms in molecules (AIM) and electron localization function (ELF) topological approaches. Chem. Rev. 105 (2005) 3911.

[45] E. Matito, M. Dura´n, M. Sola`, The aromatic fluctuation index (FLU): a new aromaticity index based on electron delocalization. J. Chem. Phys. 122 (2005) 014109.

[46] R. K. Raju, J. W. G. Bloom, Y. An, S. E. Wheeler, Substituent Effects on Non-Covalent Interactions with Aromatic Rings: Insights from Computational Chemistry. Chem. Phys. Chem. 12 (2011) 3116.

[47] R. F. W. Bader, Atoms in molecules. A Quantum Theory, Oxford University Press, Oxford (1990).

[48] D. Cremer, E. KraKa, Chemical Bonds without Bonding Electron Density-Does the Difference Electron-Density Analysis Suffice for a Description of the Chemical Bond? Angew. Chem. 23 (1984) 627.

[49] R. F. W. Bader, A quantum theory of molecular structure and its applications. Chem. Rev. 91 (1991) 893.

[50] K. Fukui, T. Yonezawa, H. Shingu, A molecular orbital theory of reactivity in aromatic hydrocarbons. J. Chem. Phys. 20 (1952) 722.

[51] K. Fukui, Role of Frontier Orbitals in Chemical Reactions. Science 218 (1982) 747.

[52] S. Gunasekaran, R. A. Balaji, S. Kumeresan, G. Anand, S. Srinivasan, Molecular and Biomolecular. Can. J. Anal. Sci. Spectrosc. 53 (2008) 149.

[53] R. G. Parr, L. Szentpaly, S. Liu, Electrophilicity Index. J. Am. Chem. Soc. 121 (1999) 1922.

[54] P. K. Chattaraj, B. Maiti, U. Sarkar, Philicity: A Unified Treatment of Chemical Reactivity and Selectivity. J. Phys. Chem. A 107 (2003) 4973.

[55] R. G. Parr, R. A. Donnelly, M. Levy, W. E. Palke, Electronegativity: the density functional viewpoint. J. Chem. Phys. 68 (1978) 3801.

[56] R. G. Parr, R. G. J. Pearson, Absolute hardness: companion parameter to absolute electronegativity. J. Am. Chem. Soc. 105 (1983) 7512.

[57] R. G. Parr, P. K. Chattraj, Principle of maximum hardness. J. Am. Chem. Soc. 113 (1991) 1854.